J. Fluid Mech. (1981), *vol.* 108, *pp.* 171–183
Printed in Great Britain

Correlated unsteady and steady laminar trailing-edge flows

By S. N. BROWN

Department of Mathematics, University College, London

AND H. K. CHENG

Department of Aerospace Engineering, University of Southern California, Los Angeles

(Received 30 May 1980)

The incompressible laminar flow in the neighbourhood of the trailing edge of an aerofoil undergoing sinusoidal oscillations of small amplitude in a uniform stream is described in the limit as the Reynolds number R tends to infinity. It is shown that if the frequency parameter is of any order less than $R^{\frac{1}{4}}$ the viscous correction to the Kutta condition and hence to the lift and moment may be determined from the results for the steady case. Justification of this correlation requires discussion of the flow in an additional region not encountered in previous studies.

1. Introduction

In this note we show that the viscous correction to the Kutta condition and hence to the lift for an aerofoil oscillating about a fixed point in a steady stream can be obtained from the corresponding results for an aerofoil at constant incidence at both moderate and fairly large values of the frequency parameter. The steady lifting aerofoil was discussed by Brown & Stewartson (1970) and the theory for a very rapidly oscillating aerofoil was given by Brown & Daniels (1975). We shall refer to these papers as I and II respectively. The correlation between the steady and unsteady flows to be described here does not hold for the high values of the frequency parameter considered in II though the theory is applicable in parts of the flow field. In both I and II extensive use was made of the trailing-edge triple-deck analysis of Stewartson (1969) and Messiter (1970).

We consider a flat plate of length l fixed at its mid-point and performing a sinusoidal pitching motion of small amplitude $\alpha^* l$ and frequency ω^*. The parameters of the problem are the Reynolds number $R = U_\infty l/\nu$, where U_∞ is the mainstream speed and ν is the kinematic viscosity, the non-dimensional amplitude α^* and the reduced frequency (or Strouhal number) $S = \omega^* l/U_\infty$. The Reynolds number is assumed to be large and the orders of magnitude of the other parameters were chosen in I and II to ensure an attached flow right up to the trailing edge. In I, the steady problem, $S = 0$ and $\alpha^* = O(R^{-\frac{1}{16}})$. In II, for the rapidly oscillating aerofoil, $S = O(R^{\frac{1}{4}})$ and $\alpha^* = O(R^{-\frac{9}{16}})$. The essential differences between these two limits, and the way in which they are spanned by the present work in which $0 < S \ll O(R^{\frac{1}{4}})$, is explained now below.

In I it is shown that the boundary layers on the two sides of the plate separately enter the triple deck and the flow in the lower deck on both sides is governed by partial differential equations which must be solved numerically for each value of

α ($= R^{\frac{1}{16}}\lambda^{-\frac{9}{8}}\alpha^*$, $\lambda = 0{\cdot}332$ the Blasius skin-friction constant). Solutions with $\alpha = 0$ were obtained by Jobe & Burggraf (1974), Veldman & van de Vooren (1975) and by Melnik & Chow (1975). The last-named authors (Chow & Melnik 1977) also considered $0 < \alpha < 0{\cdot}45$ and estimated that the flow on the suction side of the aerofoil separates precisely at the trailing edge when $\alpha = 0{\cdot}47$. In the main deck of the triple deck the velocity component u parallel to the plate is of the form

$$u(x, y)/U_\infty = \overline{U}_0(y) + R^{-\frac{1}{8}}\bar{A}(x)\, d\overline{U}_0/dy, \tag{1.1}$$

where x, y are non-dimensional distances of order unity in the triple deck measuring distances along and perpendicular to the aerofoil with origin at the trailing edge. In the limit $R \to \infty$, $\overline{U}_0(y)$ is the Blasius function. The function $\bar{A}(x)$ is determined by the solution of the inner-deck equations and an important distinction from the rapidly oscillating limit of II is that here $\bar{A}(x) = O((-x)^{\frac{1}{3}})$ as $x \to -\infty$ upstream of the triple deck. As $x \to \infty$ there is a match with a displaced Goldstein wake.

In II the partial differential equations of the inner deck of the triple deck are unsteady and no solutions of them have as yet been found though the authors did present an approximate solution for $R^{-\frac{1}{4}}S \gg 1$. The regions of flow include a perturbed Blasius layer with an underlying Stokes layer and a two-layered foredeck upstream of the conventional triple deck. The flow is unsteady in all regions and $\bar{A}(x)$ in (1.1) is now a function of the time t as well and is such that $\bar{A}(x, t) = O((-x)^{-\frac{1}{2}})$ as $x \to -\infty$ upstream of the triple deck. Again as $x \to \infty$ there is a match with a displaced Goldstein wake.

Let us now consider the intermediate values of S, i.e. $0 < S \ll O(R^{\frac{1}{4}})$. In such solutions the time derivative does not occur in the fundamental triple-deck equations and t occurs merely as a parameter. When $S = O(1)$ the perturbation to the Blasius flow differs from that for the steady case only by a factor $e^{i\omega^* t^*}$ as does the flow in the main deck of the triple deck. This means that the solution of the steady inner-deck equations applies to the unsteady case with an appropriate definition of α involving S and $e^{i\omega^* t^*}$. The same is true if the aerofoil is in a plunging rather than a pitching mode and, for sufficiently small time, to an aerofoil in a gust.

It is not immediately obvious that the numerical results of Chow & Melnik for the steady case can also be applied to the range $1 \ll S \ll R^{\frac{1}{4}}$. It is quite evident that, as when $S = O(1)$, the time derivative does not occur in the inner-deck equations, which are therefore as in I. Thus as $x \to -\infty$ the $\bar{A}(x, t)$ corresponding to $\bar{A}(x)$ in I is such that $\bar{A}(x, t) = O((-x)^{\frac{1}{3}})$. However the upstream flow is unsteady with Stokes layers in both the perturbed Blasius layer and the foredeck, which is now of width $O(S^{-1})$ instead of $O(R^{-\frac{1}{4}})$. The solutions in these regions require that for a match with the inner deck to be possible then $\bar{A}(x, t) = O((-x)^{-\frac{1}{2}})$ as $x \to -\infty$ as in the case of II with $S = O(R^{\frac{1}{4}})$. In this paper we show that this seeming mismatch can be circumvented by the insertion of a second foredeck of width $O(S^{-\frac{3}{2}})$ between the first foredeck and the triple deck. This justifies using the results of Chow & Melnik for predictions of the Kutta constant and the correction therefrom to the lift and moment for values of S from zero to any order *less* than $O(R^{\frac{1}{4}})$. The orders of magnitude of α^* and S must be such that $\alpha^* S^2 = O(R^{-\frac{1}{16}})$, unless $S \to 0$, in which case $\alpha^* = O(R^{-\frac{1}{16}})$ as in I. If the order of magnitude of this product is greater the flow will not remain attached right up to the trailing edge, and if it is less the inner-deck solution is a linear perturbation of that for the plate at zero incidence. The theory outlined in the subsequent sections embraces all values of $S < O(R^{\frac{1}{4}})$ and shows that the second foredeck merges with the triple deck as the order

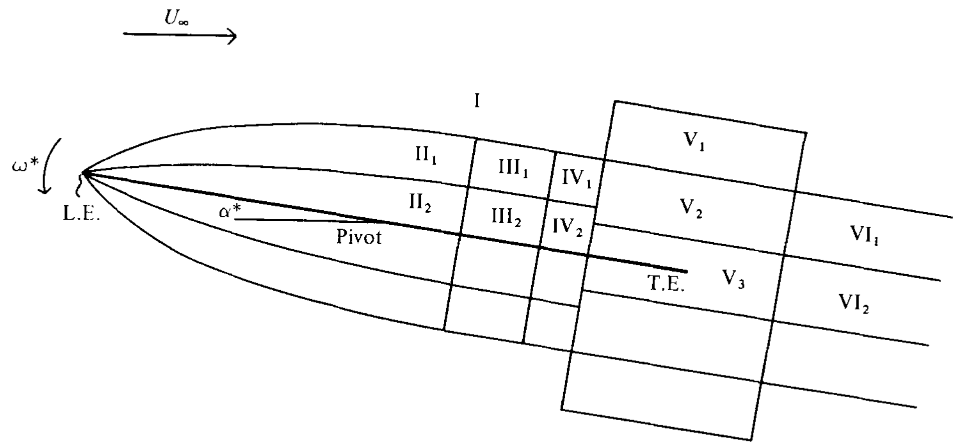

FIGURE 1. The regions of flow in the neighbourhood of the trailing edge on the upper side of the plate (not to scale). I, potential flow; II, perturbed Blasius flow and inner Stokes layer; III, the first foredeck; IV, the second foredeck; V, the triple deck; VI, modified Goldstein wake.

of magnitude of S nears $O(R^{\frac{1}{4}})$ and that as S becomes $O(1)$ the foredecks become of finite width and disappear into the perturbed Blasius layer.

The regions of flow are illustrated in figure 1. Region I is the potential flow and regions II_1 and II_2 are the perturbed Blasius layer and its Stokes layer respectively. The two layers of the first foredeck are denoted by III_1 and III_2 while the second foredeck divides into IV_1 and IV_2. Region V consists of the three layers of the triple deck while region VI comprises the outer and inner modified Goldstein wake. It is region IV that is additional to those occurring in reference II.

In the final section we apply the theory to two examples – one with $S^2 \gg 1$ and one with $S = O(1)$. We explain the method of correlation with the results of Chow & Melnik and calculate in each case the viscous correction to the lift and moment. For each example there is a maximum value of the amplitude, corresponding to the stall angle of Chow & Melnik at which separation occurred at the trailing edge. In the steady case there was a dramatic loss of lift at this angle of incidence. Here the singularity gives either an increase or decrease in the lift. In the two examples studied the phenomenon occurs at different times in the oscillatory cycle.

2. The external potential flow

The external potential flow is as set out in II though, when $S = O(1)$, (2.2) and (2.6) of that paper should be corrected as below. It reduces to that of I as $\omega^* \to 0$ though it should be noted that the limiting angle of incidence is then $2\alpha^*$ while it is α^* in I. We consider a flat plate of length l with mid-point at the origin O of a set of Cartesian co-ordinates (x^*, y^*) fixed in space. The plate performs oscillations of amplitude $\alpha^* l$ and frequency ω^* in an incompressible fluid of constant density ρ which has uniform velocity U_∞ at infinity. At any time t^* the equation of the plate is thus

$$y^* = -2\alpha^* x^* e^{i\omega^* t^*} \quad (-\tfrac{1}{2}l \leqslant x^* \leqslant \tfrac{1}{2}l), \tag{2.1}$$

where here and henceforth the real part of any complex expression is to be taken.

When terms $O(\alpha^{*2})$ are neglected the pressure on the upper surface of the plate is given by (2.2) of II corrected to read

$$\frac{p^*-p_\infty}{\rho U_\infty^2} = \tfrac{1}{2}a_0(t^*)\left(\frac{l-2x^*}{l+2x^*}\right)^{\frac{1}{2}} + \tfrac{1}{2}B(t^*)\left\{\left(\frac{l+2x^*}{l-2x^*}\right)^{\frac{1}{2}} + \Lambda(S)\left(\frac{l-2x^*}{l+2x^*}\right)^{\frac{1}{2}}\right\}$$
$$+a_1(t^*)\left(1-\frac{4x^{*2}}{l^2}\right)^{\frac{1}{2}} + 4a_2(t^*)\frac{x^*}{l}\left(1-\frac{4x^{*2}}{l^2}\right)^{\frac{1}{2}} \quad (-\tfrac{1}{2}l \leqslant x^* \leqslant \tfrac{1}{2}l), \tag{2.2}$$

where p_∞ is the pressure at infinity. The pressure on the lower side is minus the expression given in (2.2). The functions a_1, a_2 are given by

$$a_1(t^*) = -2i\alpha^* S e^{i\omega^* t^*}, \quad a_2(t^*) = \tfrac{1}{8}\alpha^* S^2 e^{i\omega^* t^*}; \tag{2.3}$$

also $B(t^*)$, which is to be found by matching with the triple deck, is related to the circulation and will give the viscous correction to the lift and moment. The function Λ is defined by

$$\Lambda(S) = \frac{H_1^{(2)}(\frac{1}{2}S) - iH_0^{(2)}(\frac{1}{2}S)}{H_1^{(2)}(\frac{1}{2}S) + iH_0^{(2)}(\frac{1}{2}S)}, \tag{2.4}$$

where $S = \omega^* l/U_\infty$ is the frequency parameter. Also $H_0^{(2)}$, $H_1^{(2)}$ are Hankel functions of the second kind, and (see Robinson & Laurmann 1956)

$$a_0(t^*) = -\alpha^* N(S)\, e^{i\omega^* t^*}, \tag{2.5}$$

where

$$N(S) = \frac{4H_1^{(2)}(\frac{1}{2}S) + SH_0^{(2)}(\frac{1}{2}S)}{H_1^{(2)}(\frac{1}{2}S) + iH_0^{(2)}(\frac{1}{2}S)}. \tag{2.6}$$

When $S \gg 1$, $\Lambda(S) \approx 0$ and

$$a_0(t^*) \approx \tfrac{1}{2}i\alpha^* S e^{i\omega^* t^*}; \tag{2.7}$$

when $S \ll 1$, the steady situation, $\Lambda(S) \approx 1$ and $a_0(t^*) \approx -4\alpha^*$.

The expressions for the lift and anti-clockwise moment in (2.6) of II should also be amended to read

$$\left.\begin{aligned} L &= -\tfrac{1}{2}\pi\rho l U_\infty^2\{a_0(t^*) + a_1(t^*) + B(t^*)\,(1+\Lambda(S))\},\\ M &= \tfrac{1}{8}\pi\rho l U_\infty^2\{a_0(t^*) - a_2(t^*) - B(t^*)\,(1-\Lambda(S))\}. \end{aligned}\right\} \tag{2.8}$$

We require the form of p^* only as the trailing edge is approached. The required expression is

$$\frac{p^*-p_\infty}{\rho U_\infty^2} = \{\tfrac{1}{2}a_0(t^*) + 2a_1(t^*) + 4a_2(t^*)\}\left(\tfrac{1}{2}-\frac{x^*}{l}\right)^{\frac{1}{2}} + \tfrac{1}{2}B(t^*)\left(\tfrac{1}{2}-\frac{x^*}{l}\right)^{-\frac{1}{2}}, \tag{2.9}$$

which reduces to that considered in I as $S \to 0$ and in II as $S \to \infty$. At this stage in I and II the orders of magnitude of the parameters were specified so that as the triple deck is approached the potential pressure in (2.9) is of the same order of magnitude as that induced by the triple deck, i.e. $O(\epsilon^2)$ when $\frac{1}{2} - x^*/l = O(\epsilon^3)$, where

$$R = U_\infty l/\nu = \epsilon^{-8} \gg 1. \tag{2.10}$$

In II this determined $\alpha^* S^2$ so that

$$\alpha^* S^2 = O(\epsilon^{\frac{1}{2}}) \tag{2.11}$$

and when $S = O(1)$ this reduces to the order of magnitude of α^* considered in I. In II S was chosen to be $O(\epsilon^{-2})$ so that the thickness of the Stokes layer underlying the perturbed Blasius boundary layer approaching the trailing edge, which is $O(S^{-\frac{1}{2}}\epsilon^4)$, was of the same order $O(\epsilon^5)$ as that of the inner deck. Here we retain (2.11) but consider any S whose order is less than ϵ^{-2} so that the Stokes layer is thicker than the inner deck, which is $O(\epsilon^5)$, but is thinner than the middle deck, which is $O(\epsilon^4)$ as is a conventional boundary layer.

If $S \ll 1$ the appropriate replacement for (2.11) is $\alpha^* = O(\epsilon^{\frac{1}{2}})$ as in I. This case is in fact covered by the situation $S = O(1)$ and the solution may be obtained by letting $S \to 0$ in the discussion of § 3.

It is instructive at this stage to compare the inviscid pressure given by (2.9) with the corresponding steady pressure obtained from (2.2) of I. In order not to confuse the notation we denote α^* and B of I by α^*_M and B_M respectively. Thus from (2.2) of I we obtain, on changing the origin there to $-\frac{1}{2}l$,

$$\frac{p^*-p_\infty}{\rho U_\infty^2} = \alpha^*_M\left\{-\left(\tfrac{1}{2}-\frac{x^*}{l}\right)^{\frac{1}{2}}+\frac{B_M}{l}\left(\tfrac{1}{2}-\frac{x^*}{l}\right)^{-\frac{1}{2}}\right\}\operatorname{sgn} y^*. \tag{2.12}$$

In the following sections we shall show that the solutions of the inner-deck equations for the steady and the unsteady problems are the same for any S with $0 < S < O(R^{\frac{1}{4}})$ if we identify α^*_M with $-\{\frac{1}{2}a_0(t^*)+2a_1(t^*)+4a_2(t^*)\}$ when this expression is positive and α^*_M with $\{\frac{1}{2}a_0(t^*)+2a_1(t^*)+4a_2(t^*)\}$ otherwise. In either case the correspondence between B_M and $B(t^*)$ is the same, namely

$$\tfrac{1}{2}B(t^*) = -\{\tfrac{1}{2}a_0(t^*)+2a_1(t^*)+4a_2(t^*)\}B_M/l, \tag{2.13}$$

and it is the determination of $B(t^*)$ that is the chief aim of the study as it gives the viscous correction to the lift and moment in (2.8). Since B_M is known as a function of α^*_M from the results of Chow & Melnik (1977) we shall be able to identify an α^*_M corresponding to each t^* and then calculate $B(t^*)$ for each t^*. If for all t^* the expression $\{\frac{1}{2}a_0(t^*)+2a_1(t^*)+4a_2(t^*)\}$ is negative then the top of the steady plate and the top of the oscillating plate correspond at all points of its cycle. If this expression changes sign then the top of the oscillating plate corresponds to the bottom of the steady plate during that time the expression is positive. When the theory has been established we shall present an example in the final section.

As in II we first non-dimensionalize the variables and change to axes fixed in the plate by writing

$$x^*/l-\tfrac{1}{2} = x+\alpha^* y e^{it}, \quad y^*/l = y-\alpha^*(x+\tfrac{1}{2})\,e^{it} \tag{2.14}$$

and

$$\left.\begin{aligned} u^*-\alpha^* v^* e^{i\omega^* t^*} &= U_\infty(u+i\alpha^* S y e^{it}),\\ \alpha^* u^* e^{i\omega^* t^*}+v^* &= U_\infty\{v-i\alpha^*(x+\tfrac{1}{2})\,e^{it}\},\end{aligned}\right\} \tag{2.15}$$

where $t = \omega^* t^*$. The equation of the plate is now

$$y = 0 \quad (-1 \leqslant x \leqslant 0) \tag{2.16}$$

for all t and as in II the extra terms in the Navier–Stokes equations due to the rotation will not be required to the degree of approximation considered.

3. The correlation between the steady and unsteady situations when $S = O(1)$

When $S = O(1)$, $\alpha^* = O(\epsilon^{\frac{1}{2}})$ and we anticipate that $B(t^*) = O(\epsilon^{\frac{7}{2}})$ as this corresponds to $B_M = O(\epsilon^3)$ in I. The flow regions are in fact exactly as outlined in I. There is a perturbed Blasius boundary layer the solution for which is, as the trailing edge is approached, identical with that in I with α^*_M replaced by

$$\alpha^*_M = \mp \{\tfrac{1}{2}a_0(t^*) + 2a_1(t^*) + 4a_2(t^*)\} \tag{3.1}$$

according as the upper surfaces of the two plates correspond or the upper surface of the steady plate corresponds to the lower surface of the oscillating plate. Again with (3.1) the solutions in the main and upper decks are the same except that the function $A_1(x)$ is replaced by $A_1(x, t)$. The equations in the inner deck are also exactly the same since the oscillation is too slow for the time derivative to occur so t is only a parameter arising in the boundary condition. The inner-deck equations have been solved by Chow & Melnik (1977) for each positive value of α^*_M up to a maximum of 0·45 for $\alpha^*_M \epsilon^{-\frac{1}{2}} \lambda^{-\frac{9}{8}}$ and we therefore have solutions for the corresponding values of t^*. In particular we have $B(t^*)$. An example is presented in § 5.

4. The steady and unsteady correlation when $S \gg 1$

(*a*) *The perturbed Blasius boundary layer and the first foredeck*

When $S \gg 1$ the perturbed Blasius boundary layer that approaches the trailing edge has an underlying Stokes layer of thickness $\epsilon^4 S^{-\frac{1}{2}}$. The solution is exactly that given in II, which we rewrite, without stipulating the order of magnitude of S, as

$$\left.\begin{aligned} u &= f'_B(\zeta) - \tfrac{1}{4}i\alpha^* S(-x)^{-\frac{1}{2}}\, e^{it}, \\ \bar{v} &= -\tfrac{1}{2}(1+x)^{-\frac{1}{2}}\,(f_B - \zeta f'_B) + \tfrac{1}{8}i\alpha^* S\bar{y}(-x)^{-\frac{3}{2}}\, e^{it}, \end{aligned}\right\} \tag{4.1}$$

to the required degree of approximation. Here

$$\bar{y} = y/\epsilon^4, \quad \bar{v} = v/\epsilon^4, \quad \zeta = \bar{y}/(1+x)^{\frac{1}{2}}, \tag{4.2}$$

where u, v are the velocity components defined in (2.15) and $f_B(\zeta)$ is the Blasius function.

In the Stokes region below this

$$\bar{y} = S^{-\frac{1}{2}} z \tag{4.3}$$

and

$$\left.\begin{aligned} u &= \lambda S^{-\frac{1}{2}}(1+x)^{-\frac{1}{2}}\, z - \tfrac{1}{4}i\alpha^* S(-x)^{-\frac{1}{2}}\,(1 - e^{-i^{\frac{1}{2}}z})\, e^{it}, \\ \tilde{v} &= \tfrac{1}{4}\lambda S^{-1}(1+x)^{-\frac{3}{2}}\, z^2 + \tfrac{1}{8}i\alpha^* S^{\frac{1}{2}}(-x)^{-\frac{3}{2}}\,\{z - i^{-\frac{1}{2}}(1 - e^{-i^{\frac{1}{2}}z})\}\, e^{it}, \end{aligned}\right\} \tag{4.4}$$

where $i^{\frac{1}{2}} = (1+i)/2^{\frac{1}{2}}$.

The next region encountered by the fluid is the foredeck, which is of width $O(S^{-1})$. In II it was of width $O(\epsilon^2)$ since there S^{-1} was $O(\epsilon^2)$ and the solution here is exactly the same. The only result we shall need from this is the behaviour of the solution as the fluid leaves this deck on the trailing-edge side. From II this is found to be

$$\left.\begin{aligned} u &= U_0(\bar{y}) - \tfrac{1}{4}i\alpha^* S^{\frac{3}{2}}\lambda^{-1}(-x_1)^{-\frac{1}{2}}\, U'_0(\bar{y})\, e^{it}, \\ \tilde{v} &= \tfrac{1}{8}i\alpha^* S^{\frac{5}{2}}\lambda^{-1}(-x_1)^{-\frac{3}{2}}\, U_0(\bar{y})\, e^{it} \quad (x_1 \to 0^-), \end{aligned}\right\} \tag{4.5}$$

where $x_1 = Sx$ and $U_0(\bar{y}) = f'_B(\bar{y})$, the Blasius profile evaluated at the trailing edge.

In the lower deck of the foredeck the solution is as (4.3), (4.4) written in terms of x_1. It is at this stage we find that we are going to be unable to effect a match between the foredeck and the Stewartson triple deck as described in I. The required power of x_1 for a match of the velocity component u will be $(-x_1)^{\frac{1}{6}}$ since the steady equations will hold in the triple deck with t simply playing the role of a parameter. This indicates the presence of a second foredeck between this and the triple deck, its width being determined by the requirement that the perturbation to u, which in terms of the original x enters the second foredeck with order of magnitude $O(\alpha^* S(-x)^{-\frac{1}{2}})$ as in (4.5), leaves it with an order of magnitude $O(\alpha^* S^2(-x)^{\frac{1}{6}})$. This last order of magnitude is deduced from the behaviour of the triple-deck flow on the upstream side as discussed in I. There the factor S^2 was of course absent but is present here because the dominant term in the inviscid pressure, which forces the term in $(-x)^{\frac{1}{6}}$, is, when $S \gg 1$, the contribution from $a_2(t^*)$ in (2.9), which is, from (2.3), proportional to $\alpha^* S^2$. In I the corresponding term was simply $O(\alpha^*)$. The requirement that the two orders of magnitude, $O(\alpha^* S(-x)^{-\frac{1}{2}})$ and $O(\alpha^* S^2(-x)^{\frac{1}{6}})$, be the same leads to

$$x = O(S^{-\frac{3}{2}}) \tag{4.6}$$

as the width of the second foredeck. The success of the present scheme depends on their being an appropriate solution in the new deck. We justify it in the following.

(*b*) *The second foredeck*

The crucial region that provides the match between the essentially unsteady flow in the perturbed Blasius layer and foredeck and the steady triple deck is, as shown in the previous section, of width $O(S^{-\frac{3}{2}})$. Like the regions considered previously it is in two parts, one of thickness $O(\epsilon^4)$ and the second, as will emerge, of thickness $O(\epsilon^4 S^{-\frac{1}{2}})$ as the Stokes layers previously considered. In the second foredeck the pressure is still determined by the inviscid solution and the equations that hold are again the boundary-layer equations

$$\frac{\partial u}{\partial x}+\frac{\partial \bar{v}}{\partial \bar{y}} = 0, \quad S\frac{\partial u}{\partial t}+u\frac{\partial u}{\partial x}+\bar{v}\frac{\partial u}{\partial \bar{y}} = \tfrac{1}{4}\alpha^* S^2(-x)^{-\frac{1}{2}}\,e^{it}+\frac{\partial^2 u}{\partial \bar{y}^2}. \tag{4.7}$$

In this region the mainstream is of the form $U_\infty\{1+U(x)\,e^{it}\}$, where $U(x)$ is determined from $U_\infty U'(x) = -p^{*\prime}(x)/\rho$, so that, from (2.9) with $S \gg 1$,

$$U(x) = -\tfrac{1}{2}\alpha^* S^2(-x)^{\frac{1}{2}}. \tag{4.8}$$

In (4.7) we write $x_2 = S^{\frac{3}{2}}x$ and

$$\left.\begin{aligned} u &= U_0(\bar{y})+\alpha^* S^{\frac{7}{4}} u_2(x_2,\bar{y})\,e^{it}, \\ \bar{v} &= \alpha^* S^{\frac{13}{4}} v_2(x_2,\bar{y})\,e^{it}, \end{aligned}\right\} \tag{4.9}$$

the powers of S following from (4.5) written in the variable x_2. Then we obtain

$$\left.\begin{aligned} iu_2+S^{\frac{1}{2}}U_0(\bar{y})\frac{\partial u_2}{\partial x_2}+S^{\frac{1}{2}}U_0'(\bar{y})\,v_2 &= \tfrac{1}{4}(-x_2)^{-\frac{1}{2}}+S^{-1}\frac{\partial^2 u_2}{\partial \bar{y}^2}, \\ \frac{\partial u_2}{\partial x_2}+\frac{\partial v_2}{\partial \bar{y}} &= 0. \end{aligned}\right\} \tag{4.10}$$

The solution of (4.10), is, since $S \gg 1$,

$$u_2 = A_2(x_2)\,U_0'(\bar{y}), \quad v_2 = -A_2'(x_2)\,U_0(\bar{y}), \tag{4.11}$$

where $A_2(x_2)$ is determined by the solution in the lower deck of the foredeck which we now consider.

In this lower deck we write

$$\bar{y} = S^{-\frac{1}{2}}\bar{y}_2, \quad v_2 = S^{-\frac{1}{2}}\bar{v}_2, \tag{4.12}$$

so that equations (4.10) become

$$\left.\begin{aligned} \frac{i}{\lambda}u_2 + \bar{y}_2\frac{\partial u_2}{\partial x_2} + \bar{v}_2 &= \frac{1}{4\lambda}(-x_2)^{-\frac{1}{2}} + \frac{1}{\lambda}\frac{\partial^2 u_2}{\partial \bar{y}_2^2}, \\ \frac{\partial u_2}{\partial x_2} + \frac{\partial \bar{v}_2}{\partial \bar{y}_2} &= 0, \end{aligned}\right\} \tag{4.13}$$

where $\lambda = U_0'(0) = 0{\cdot}332$. These equations are to be solved over $(-\infty, 0)$ such that $u_2(x_2, 0) = \bar{v}_2(x_2, 0) = 0$ and $u_2 \to \lambda A_2(x_2)$ as $\bar{y}_2 \to \infty$. Since the equations are parabolic, so that the solution in $x_2 < 0$ is unaffected by that in $x_2 > 0$, we may assume that they and the boundary conditions hold for all x_2 with the function $(-x_2)^{-\frac{1}{2}}$ defined to be zero for $x_2 > 0$. Thus we may use a Fourier transform and define $\tilde{u}_2(\omega, y_2)$ as the Fourier transform of $u_2(x_2, y_2)$ with respect to x_2 so that

$$\tilde{u}_2(\omega, \bar{y}_2) = \int_{-\infty}^{\infty} u_2(x_2, \bar{y}_2)\, e^{-i\omega x_2}\, dx_2 \tag{4.14}$$

and find that the solution of (4.13) satisfying the boundary conditions at $\bar{y}_2 = 0$ is

$$\frac{\partial \tilde{u}_2}{\partial \bar{y}_2} = -\frac{\pi^{\frac{1}{2}}}{4\lambda^{\frac{1}{3}}}\frac{e^{i\pi/12}\,\mathrm{Ai}\,(Z_1)}{(\omega + i\delta)^{\frac{1}{2}}\,(\omega - i\delta)^{\frac{1}{3}}\,\mathrm{Ai}'\,(Z_0)}. \tag{4.15}$$

Here

$$Z_1 = \frac{\lambda^{\frac{1}{3}}\, e^{i\pi/6}(\lambda^{-1} + \omega\bar{y}_2)}{(\omega - i\delta)^{\frac{2}{3}}}, \quad Z_0 = \frac{e^{i\pi/6}}{\lambda^{\frac{2}{3}}(\omega - i\delta)^{\frac{2}{3}}} \tag{4.16}$$

and δ is a small parameter introduced for convenience. The transform $\tilde{A}_2(\omega)$ of $A_2(x_2)$ is determined by the requirement that $u_2 \to \lambda A_2(x_2)$ as $\bar{y}_2 \to \infty$. This leads to

$$\tilde{A}_2(\omega) = -\frac{\pi^{\frac{1}{2}}\, e^{-i\pi/12}}{4\lambda^{\frac{2}{3}}\,\mathrm{Ai}'\,(Z_0)}(\omega + i\delta)^{-\frac{1}{2}}\,(\omega - i\delta)^{-\frac{2}{3}} \int_{Z_0}^{\infty} \mathrm{Ai}\,(Z_1)\, dZ_1. \tag{4.17}$$

It now remains to check that this foredeck solution does what is required of it. In fact the behaviour of u_2 and $\partial u_2/\partial \bar{y}_2$ therein is very similar to that of the corresponding quantities in the perturbed Blasius boundary layer of I of which this is the unsteady analogue. To ensure that we have a match with the foredeck we must examine this solution as $x_2 \to -\infty$. The easiest quantity to examine is the skin friction, which must match with that given by (4.4), which also holds throughout the foredeck. We consider (4.15) for small $|\omega|$ from which, on replacing the Airy functions by their asymptotic expansions,

$$\left.\frac{\partial \tilde{u}_2}{\partial \bar{y}_2}\right)_{\bar{y}_2=0} \approx \tfrac{1}{4}\pi^{\frac{1}{2}}(\omega + i\delta)^{-\frac{1}{2}}, \tag{4.18}$$

so that, as $x_2 \to -\infty$,

$$\left.\frac{\partial u_2}{\partial \bar{y}_2}\right)_{\bar{y}_2=0} \approx \tfrac{1}{4}e^{-\frac{1}{4}i\pi}(-x_2)^{-\frac{1}{2}}, \tag{4.19}$$

which leads to a match with the second term of (4.4).

We now require the form of $A_2(x_2)$ as $x_2 \to 0^-$ to see if we can match with the known properties of the steady triple deck as discussed in I. The behaviour of $A_2(x_2)$ as $x_2 \to 0^-$ may be obtained by considering $|\omega|$ to be large in (4.17). Thus

$$\tilde{A}_2(\omega) \approx -\frac{\pi^{\frac{1}{2}}\lambda^{-\frac{5}{3}}}{12\,\mathrm{Ai}'(0)}\, e^{-i\pi/12}(\omega+i\delta)^{-\frac{1}{2}}\,(\omega-i\delta)^{-\frac{2}{3}} \tag{4.20}$$

so that, upon inversion,

$$A_2(x_2) \approx -\frac{6^{\frac{1}{3}}(-\frac{1}{3})!}{2\lambda^{\frac{5}{3}}}(-x_2)^{\frac{1}{6}} \quad \text{as} \quad x_2 \to 0^-, \tag{4.21}$$

and the required one-sixth power for a match with the steady triple-deck solution is recovered.

Again as in the perturbed Blasius boundary-layer discussion of I the behaviour of $\partial u_2/\partial \bar{y}_2)_{\bar{y}_2=0}$ is non-commutative as $-x_2 \to 0$. If we let $\bar{y}_2 \to 0$ first we obtain, from (4.15),

$$\left.\frac{\partial \tilde{u}_2}{\partial \bar{y}_2}\right)_{\bar{y}_2=0} \approx -\frac{\pi^{\frac{1}{2}}\,e^{i\pi/12}\,\mathrm{Ai}\,(0)}{4\lambda^{\frac{1}{3}}\,\mathrm{Ai}'\,(0)}\,(\omega+i\delta)^{-\frac{1}{2}}\,(\omega-i\delta)^{-\frac{1}{3}}, \tag{4.22}$$

on subsequently considering $|\omega|$ to be small, which on inversion leads to

$$\left.\frac{\partial u_2}{\partial \bar{y}_2}\right)_{\bar{y}_2=0} \approx \frac{6^{-\frac{1}{3}}\lambda^{-\frac{1}{3}}}{2}\left[\frac{(-\frac{2}{3})!}{(-\frac{1}{3})!}\right]^2(-x_2)^{-\frac{1}{6}}. \tag{4.23}$$

However, if we let $x_2 \to 0$ first we find that

$$\left.\frac{\partial u_2}{\partial \bar{y}_2}\right)_{x_2=0} = -\frac{\pi^{-\frac{1}{2}}\,e^{i\pi/12}}{8\lambda^{\frac{1}{3}}}\int_{-\infty}^{\infty}\frac{\mathrm{Ai}\,(Z_1)\,d\omega}{(\omega+i\delta)^{\frac{1}{2}}\,(\omega-i\delta)^{\frac{1}{3}}\,\mathrm{Ai}'\,(Z_0)}, \tag{4.24}$$

which is to be examined as $\bar{y}_2 \to 0$. For small $\bar{y}_2$ the chief contribution to the integral comes from large values of $|\omega|$ and it is sufficient to consider

$$\left.\frac{\partial u_2}{\partial \bar{y}_2}\right)_{x_2=0} \approx -\frac{\pi^{-\frac{1}{2}}\,e^{i\pi/12}}{8\lambda^{\frac{1}{3}}\,\mathrm{Ai}'\,(0)}\int_{-\infty}^{\infty}\frac{\mathrm{Ai}\,[e^{i\pi/6}(\omega-i\delta)^{\frac{1}{3}}\,\lambda^{\frac{1}{3}}\,\bar{y}_2]\,d\omega}{(\omega+i\delta)^{\frac{1}{2}}\,(\omega-i\delta)^{\frac{1}{3}}}. \tag{4.25}$$

Now the integral in (4.25) may be shown to be equal to

$$\begin{aligned} 2e^{-i\pi/12}\int_0^{\infty}\frac{\mathrm{Ai}\,(\tau^{\frac{1}{3}}\,\lambda^{\frac{1}{3}}\,\bar{y}_2)}{\tau^{\frac{5}{6}}}\,d\tau &= \frac{2e^{-i\pi/12}}{\pi}\mathrm{Re}\int_0^{\infty}\int_0^{\infty}\frac{\exp\,(\frac{1}{3}is^3+i\tau^{\frac{1}{3}}\lambda^{\frac{1}{3}}\,\bar{y}_2 s)}{\tau^{\frac{5}{6}}}\,d\tau\,ds \\ &= 3^{\frac{1}{6}}\pi^{-\frac{1}{2}}\lambda^{-\frac{1}{6}}e^{-i\pi/12}(-\tfrac{5}{6})!\,\bar{y}_2^{-\frac{1}{2}}. \end{aligned} \tag{4.26}$$

So altogether

$$\left.\frac{\partial u_2}{\partial \bar{y}_2}\right)_{x_2=0} \approx \frac{3^{\frac{1}{2}}(-\frac{2}{3})!\,(-\frac{5}{6})!}{8\pi\lambda^{\frac{1}{2}}\bar{y}_2^{\frac{1}{2}}} \quad \text{as} \quad \bar{y}_2 \to 0. \tag{4.27}$$

This solution has the same form as that in the perturbed Blasius boundary layer of I and may be matched directly to the steady triple deck with an appropriate definition of α^*_M. In the second foredeck we see that the combination $\bar{y}_2/(-x_2)^{\frac{1}{3}}$ is equal to $\bar{y}/(-x)^{\frac{1}{3}}$, the variable that is $O(1)$ in the scaled co-ordinates of the triple deck.

As S increases to $O(\epsilon^{-2})$ the second foredeck becomes identical with the triple deck and the flow therein is unsteady. As S decreases to become $O(1)$ both foredecks become of finite width and are indistinguishable from the Blasius boundary layer.

This completes the theoretical discussion of the correspondence between the steady and unsteady trailing-edge flows. We now present two examples, one with $S \gg 1$ and the second with $S = O(1)$.

5. Two examples of the viscous correction to the unsteady lift and moment

(*a*) $S \gg 1$

When $S \gg 1$ we replace a_0, a_1, a_2 in (2.8), (2.9) by their values for large S so that (2.8) becomes

$$\left.\begin{aligned} L &= -\tfrac{1}{2}\pi\rho l U_\infty^2\{\tfrac{3}{2}\alpha^* S \sin t + B(t^*)\}, \\ M &= -\tfrac{1}{8}\pi\rho l U_\infty^2\{\tfrac{1}{8}\alpha^* S^2 \cos t + B(t^*)\}, \end{aligned}\right\} \tag{5.1}$$

and, since $\tfrac{1}{2}a_0(t^*) + 2a_1(t^*) + 4a_2(t^*) \approx \tfrac{1}{2}\alpha^* S^2 \cos t$, the correspondence between α_M^* of the steady situation and α^* here is, as explained following (2.12),

$$\alpha_M^* = \mp \tfrac{1}{2}\alpha^* S^2 \cos t, \tag{5.2}$$

according as $\cos t$ I 0. Also in the notation of $\lesseqgtr$, and Melnik & Chow (1975),

$$B_M/l = \epsilon^3 \lambda^{-\frac{5}{4}} a_1(\alpha_M),$$

where $\alpha_M^* = \epsilon^{\frac{1}{2}}\lambda^{\frac{9}{8}}\alpha_M$. Hence equation (2.13) gives for $B(t^*)$

$$B(t^*) = -\alpha^* S^2 \epsilon^3 \lambda^{-\frac{5}{4}} a_1(\alpha_M) \cos t, \tag{5.3}$$

where α_M varies with t according to (5.2). Between them (5.2) and (5.3) determine $B(t^*)$ and from (5.1) we have

$$L = \tfrac{1}{2}\pi\rho l U_\infty^2 \alpha^* S^2\{-\tfrac{3}{2}S^{-1}\sin t + \epsilon^3\lambda^{-\frac{5}{4}} b_1(t)\cos t\}, \tag{5.4}$$

$$M = \tfrac{1}{8}\pi\rho l U_\infty^2 \alpha^* S^2\{-\tfrac{1}{8} + \epsilon^3\lambda^{-\frac{5}{4}} b_1(t)\}\cos t, \tag{5.5}$$

where $b_1(t) = a_1(\alpha_M)$. Thus the viscous correction to the lift is greater by a factor of S than that to the moment.

From equation (5.2) we see that when $\cos t > 0$, i.e. when the oscillating plate has a positive incidence to the oncoming flow, its upper surface corresponds to the lower surface of the steady aerofoil. Now the maximum value of α_M is 0·47 corresponding to the separation of the flow on the top of the steady plate, so if as an example we choose

$$\tfrac{1}{2}\alpha^* S^2 = 0{\cdot}47\epsilon^{\frac{1}{2}}\lambda^{\frac{9}{8}} \tag{5.6}$$

then the flow will just separate at the trailing edge every time $\cos t = \pm 1$. We use the results of Chow & Melnik, who graphed $a_1(\alpha_M)$ for $0 \leqslant \alpha_M \leqslant 0{\cdot}45$ and estimated separation to occur at $\alpha_M = 0{\cdot}47$, to plot $b_1(t)\cos t$ for this example in figure 2. If as a representative period we take $0 \leqslant t \leqslant 2\pi$ we see that for the first quarter period the aerofoil is at a positive incidence to the oncoming flow since $\cos t > 0$ but, as the lower surface of the plate corresponds to the upper surface of the steady aerofoil, the separation that occurs at $t = 0$ is on the lower surface and corresponds to a dramatic increase rather than decrease of lift. At $t = \pi$ the flow just separates on the upper surface when the aerofoil is at its maximum negative incidence to the oncoming stream and there is a decrease of lift. At $t = 2\pi$ the separation is on the lower surface again. At $t = 0$ and 2π there is a considerable increase in clockwise moment and at $t = \pi$ a decrease.

In figure 2 we also include $b_1(t)\cos t$ for the example

$$\tfrac{1}{2}\alpha^* S^2 = 0{\cdot}235\epsilon^{\frac{1}{2}}\lambda^{\frac{9}{8}} \tag{5.7}$$

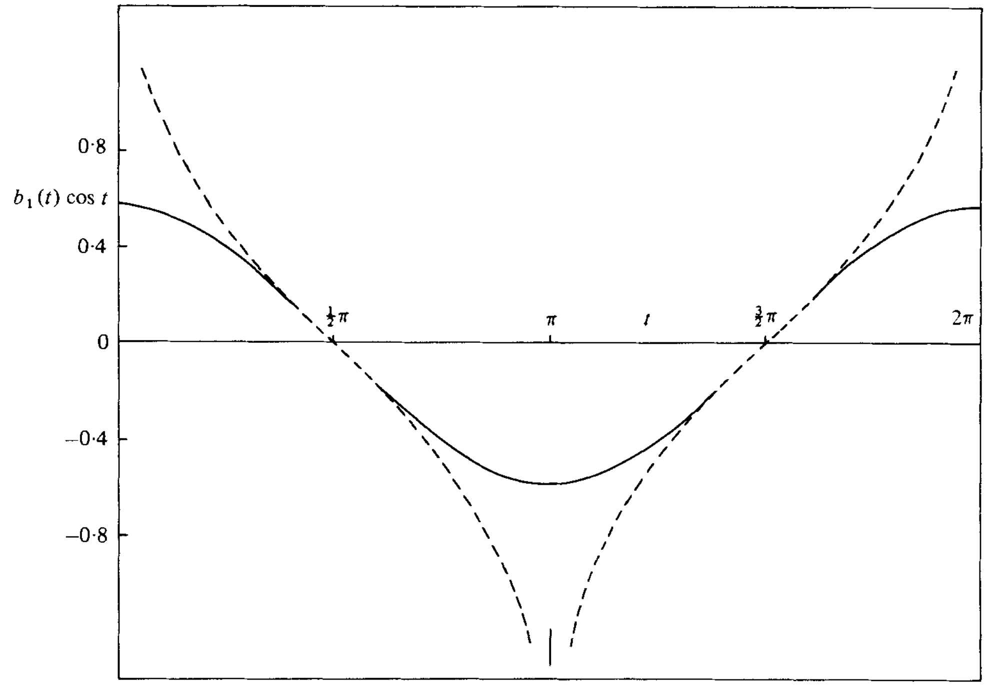

FIGURE 2. The function $b_1(t)\cos t$ for $S \gg 1$ and $\frac{1}{2}\alpha^* S^2 = 0{\cdot}47\epsilon^{\frac{1}{2}}\lambda^{\frac{9}{8}}$ (broken curve) and $\frac{1}{2}\alpha^* S^2 = 0{\cdot}235\epsilon^{\frac{1}{2}}\lambda^{\frac{9}{8}}$ (continuous curve).

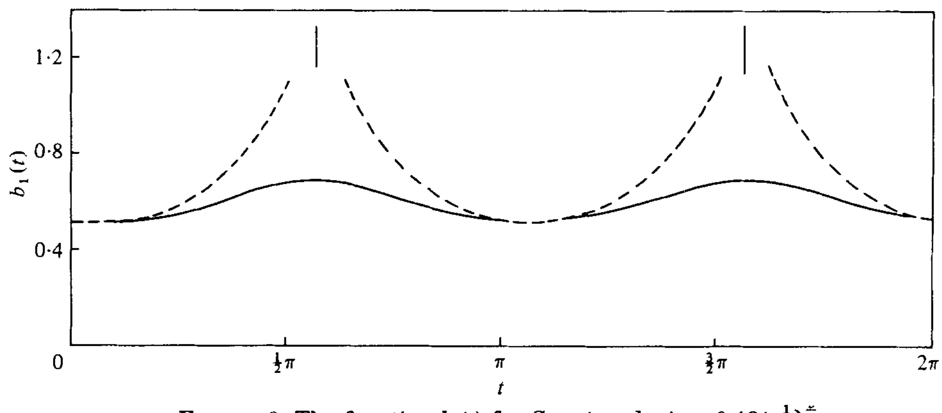

FIGURE 3. The function $b_1(t)$ for $S = 1$ and $\alpha^* = 0{\cdot}131\epsilon^{\frac{1}{2}}\lambda^{\frac{9}{8}}$ (broken curve) and $\alpha^* = 0{\cdot}098\epsilon^{\frac{1}{2}}\lambda^{\frac{9}{8}}$ (continuous curve).

for which the amplitude is never so large as to cause separation. This is illustrated by the smoothness of the curve.

(*b*) $S = O(1)$

For the second example we set $S = 1$ so that now

$$\frac{\alpha_M^*}{\alpha^*} = \pm \operatorname{Re}\{\tfrac{1}{2}N(1) + 4i - \tfrac{1}{2}\}\, e^{it} \tag{5.8}$$

according as the right-hand side is positive or negative, and (2.13) gives

$$B(t^*) = \operatorname{Re}\alpha^* \epsilon^3 \lambda^{-\frac{5}{4}} a_1(\alpha_M)\{N(1) + 8i - 1\}\, e^{it}. \tag{5.9}$$

From (2.8) we now obtain

$$L = \mathrm{Re}\,\tfrac{1}{2}\pi\rho l U_\infty^2 \alpha^*\{N(1)+2i-(1+\Lambda(1))\,\epsilon^3\lambda^{-\frac{5}{4}}b_1(t)\,(N(1)+8i-1)\}\,e^{it}, \qquad (5.10)$$

$$M = -\mathrm{Re}\,\tfrac{1}{8}\pi\rho l U_\infty^2 \alpha^*\{N(1)+\tfrac{1}{8}+(1-\Lambda(1))\,\epsilon^3\lambda^{-\frac{5}{4}}b_1(t)\,(N(1)+8i-1)\}\,e^{it}, \qquad (5.11)$$

where, as before, $b_1(t) = a_1(\alpha_M)$, to be calculated from (5.8) and the results of Melnik & Chow.

Since (5.8) may be written as

$$\alpha_M^*/\alpha^* = \pm\,(0{\cdot}771\cos t - 3{\cdot}498\sin t) \qquad (5.12)$$

and the maximum of the expression on the right-hand side is 3·582 occurring when $t = 1{\cdot}788$, we take

$$\alpha^* = 0{\cdot}131\epsilon^{\frac{1}{2}}\lambda^{\frac{9}{8}} \qquad (5.13)$$

so that $\max \alpha_M = 0{\cdot}47$. In figure 3 we plot $b_1(t)$ (not $b_1(t)\cos t$ as in figure 2) and note that separation occurs at $t = 1{\cdot}788$, $t = 4{\cdot}929$. At $t = 0$ the aerofoil is at maximum amplitude in the nose-up position and the upper surface of this aerofoil corresponds to the upper surface of the steady aerofoil until $t = 0{\cdot}217$. Thus the first separation, which occurs at $t = 1{\cdot}788$, by which time the aerofoil is in the the nose-down position and at about $\frac{1}{5}$ of its maximum deviation, is on the lower side of the plate. The expressions (5.10), (5.11) for the lift and anti-clockwise moment about the mid-point become, for this example,

$$L = \tfrac{1}{2}\pi\rho l U_\infty^2 \alpha^*\{2{\cdot}542\cos t - 0{\cdot}995\sin t - \epsilon^3\lambda^{-\frac{5}{4}}b_1(t)\,(3{\cdot}953\cos t - 7{\cdot}901\sin t)\}, \qquad (5.14)$$

$$M = -\tfrac{1}{8}\pi\rho l U_\infty^2 \alpha^*\{2{\cdot}667\cos t + 1{\cdot}005\sin t - \epsilon^3\lambda^{-\frac{5}{4}}b_1(t)\,(0{\cdot}868\cos t + 6{\cdot}090\sin t)\}, \qquad (5.15)$$

so this separation corresponds to an increase of lift and anti-clockwise moment. The second separation in $0 \leqslant t \leqslant 2\pi$ occurs when $t = 4{\cdot}929$ and the aerofoil is in the nose-up position. This is now on the upper side of the plate and gives a dramatic decrease in lift and anti-clockwise moment.

Also in figure 3 we include $b_1(t)$ for the example

$$\alpha^* = 0{\cdot}098\epsilon^{\frac{1}{2}}\lambda^{\frac{9}{8}}, \qquad (5.16)$$

for which the flow does not separate at any part of the cycle. The expressions for the lift and moment are again (5.14), (5.15).

6. Conclusions

We have shown how the viscous correction to the lift and moment for an aerofoil oscillating in a uniform incompressible main stream may be calculated from the results of Chow & Melnik (1977) for the steady case as long as the frequency of oscillation is not too large, specifically $S \ll R^{\frac{1}{4}}$. A similar analysis can be carried through when the aerofoil is in a plunging rather than a pitching mode with

$$y^* = -\tfrac{1}{2}h^* l\cos\omega^* t^* \quad (-\tfrac{1}{2}l \leqslant x^* \leqslant \tfrac{1}{2}l) \qquad (6.1)$$

though the values of $a_0(t^*)$, $a_1(t^*)$, $a_2(t^*)$ are now different. We have presented examples for an oscillating aerofoil both when $S = 1$ and $S \gg 1$ which illustrate the correction to the lift and moment for an amplitude when the flow just separates at the trailing edge and again when there is no separation at any point of the cycle. Such separation is often interpreted as trailing-edge stall.

This work was in part supported by the U.S. National Science Foundation, Engineering Division.

REFERENCES

BROWN, S. N. & DANIELS, P. G. 1975 On the viscous flow about the trailing edge of a rapidly oscillating plate. *J. Fluid Mech.* **67**, 743–761.

BROWN, S. N. & STEWARTSON, K. 1970 Trailing-edge stall. *J. Fluid Mech.* **42**, 561–584.

CHOW, R. & MELNIK, R. E. 1977 Numerical solutions of the triple-deck equations for laminar trailing-edge stall. *Proc. 5th Int. Conf. on Numerical Methods in Fluid Dyn.*, Lecture Notes in Physics, vol. 59, pp. 135–144. Springer.

JOBE, C. E. & BURGGRAF, O. R. 1974 The numerical solutions of the asymptotic equation of trailing-edge flow. *Proc. Roy. Soc.* A **340**, 91–111.

MELNIK, R. E. & CHOW, R. 1975 Asymptotic theory of two-dimensional trailing-edge flows. Presented at NASA Conf. on 'Aerodynamic analysis requiring advanced computers'.

MESSITER, A. F. 1970 Boundary-layer flow near the trailing edge of a flat plate. *S.I.A.M. J. Appl. Math.* **18**, 241–257.

ROBINSON, A. & LAURMANN, J. A. 1956 *Wing Theory.* Cambridge University Press.

STEWARTSON, K. 1969 On the flow near the trailing edge of a flat plate II. *Mathematika* **16**, 106–121.

VELDMAN, A. E. P. & VAN DE VOOREN, A. I. 1974 Drag of a finite plate. *Proc. 4th Int. Conf. on Numerical Methods in Fluid Dyn.*, Lecture Notes in Physics, vol. 35, pp. 422–430. Springer.